

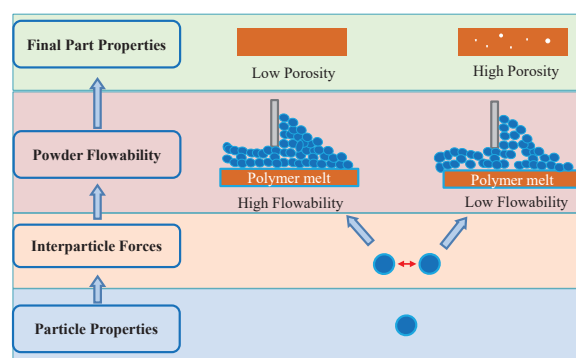
Role of Powder Properties and Flowability in Polymer Selective Laser Sintering—A Review[†]

Xi Guo and Brij M. Moudgil*

Department of Materials Science and Engineering, Center for Particulate and Surfactant Systems (CPaSS), University of Florida, USA

Polymer selective laser sintering (SLS) is an additive manufacturing technology that involves the melting of a selected area of particles on the powder bed. A 3D component is then printed using layer-by-layer sintering of the powder bed. SLS is considered one of the most promising technologies applicable to a variety of applications, particularly for manufacturing customized design products with high geometric complexity, such as patient-specific designed implants, surgical tools. Currently, only a small number of polymers are available that are suitable for SLS due to the complex multiple physical phenomena involved. Therefore, it is critical to develop new materials in order to fully realize the potential of SLS technology for manufacturing value-added customized products. For a given material, the quality of powder spreading in SLS plays a key role in printing performance and is a precondition for new material development. The aim of this review is to (1) present flowability characterization methods suitable for SLS, (2) examine the influence of powder properties and flowability on laser–material interaction and the quality of the final part, and (3) discuss the methods adopted in the literature to improve the quality of powder spreading.

Keywords: polymer selective laser sintering, powder property, flowability, powder packing



1. Introduction

Additive manufacturing (AM) is a group of solid freeform fabrication methods used to build 3D objects layer by layer based on computer-aided design files. The layer-by-layer building process, which is the opposite of traditional subtractive manufacturing, enables additive manufacturing to create highly complex structures. AM was introduced in the late 1980s (Ligon et al., 2017), primarily for building complex structure prototypes. With the development of technology, AM nowadays is capable of building products with various materials (polymers, metals, ceramics), processing desired properties and shapes.

The fundamental principle of AM process is to form parts by joining materials together. In polymer additive manufacturing, this is achieved through thermal reaction or chemical reaction, or both. Current processes in polymer AM include material extrusion, material jetting, powder bed fusion, binder jetting, vat photopolymerization, and sheet lamination (ISO/ASTM, 2021). In selective laser sintering (SLS), a laser is used to selectively melt or fuse particles in the powder bed, layer by layer. SLS is one of

the most widely used AM technologies due to its high level of accuracy, high productivity in manufacturing complex structures, and good mechanical properties (Kruth et al., 1998; Lupone et al., 2022).

To address the unmet needs in various industries, researchers have investigated the processability of several polymers including Polyamides (PA) (Beitz et al., 2019; Benedetti et al., 2019; Berretta et al., 2014; Drummer et al., 2010; Soe, 2012; Starr et al., 2011; Vasquez et al., 2011, 2014), Polypropylene (Ituarte et al., 2018; Kleijnen et al., 2016, 2017; Tan et al., 2021; Wegner, 2016; Zhu et al., 2016), Polyetheretherketone (PEEK) (Benedetti et al., 2019; Berretta et al., 2014, 2016), Polyethylene (Drummer et al., 2010), Polyoxymethylene (Drummer et al., 2010), Poly-butylene terephthalate (Schmidt et al., 2016), Poly-ε-caprolactone (Williams et al., 2005), Polystyrene (Yan et al., 2011), Thermoplastic polyurethanes (Dadbakhsh et al., 2016; Vasquez et al., 2014; Verbelen et al., 2017; Yuan et al., 2017), Thermoplastic elastomers (Vasquez et al., 2014), etc. However, it is worth noting that the SLS process currently has a limited number of commercially available polymers. PA-related materials account for over 95 % of the market (Goodridge and Ziegelmeier, 2017; Stansbury and Idacavage, 2016). Semi-crystalline polymers such as Polyamide 12 (PA12) are the material of choice in SLS for the following reasons, (1) sharp melting peak to ensure homogeneous melting, (2) large melting temperature (T_m)

[†] Received 25 July 2022; Accepted 22 September 2022
J-STAGE Advance published online 29 July 2023

* Corresponding author: Brij M. Moudgil;
Add: Gainesville, FL 32611, USA
E-mail: bmoudgil@perc.ufl.edu
TEL: +1-352-846-1194 Fax: +1-352-846-1196

to degradation temperature (T_d) window to enable full melting, (3) a rapid viscosity drop once the crystalline region disappears enabling rapid particle coalescence (Drummer et al., 2010). The limited material option is a result of the high powder production cost, lower final part mechanical properties, and dimensional accuracy compared to the traditional manufacturing processes.

The physical phenomena involved in SLS include particle spreading and deposition, laser material interaction, polymer melting and coalescence, and polymer crystallization. Each phenomenon spans different time scales and has a significant impact on the final product properties (Bierwisch et al., 2021; Lupone et al., 2022). An in-depth understanding of these phenomena is the key to improving the final part properties and expanding the suitability of commercial powders for SLS applications.

A SLS process schematic and a process temperature profile are depicted in Fig. 1. The process temperature profile is embedded in a semi-crystalline polymer differential scanning calorimetry (DSC) graph to provide a better understanding of polymer heating and cooling behavior during SLS.

The SLS process initiates with a preheating step. An inert gas is continuously purged into the printing chamber from this step and throughout the entire printing process. As shown in Fig. 1 diagram A, the polymer powder on the powder bed is preheated to a temperature below the polymer's T_m . This temperature is defined as the printing temperature. The preheating step holds significant importance for several reasons: (1) it stabilizes the temperature of the entire instrument, (2) it minimizes the energy required for melting the polymer in the target area, (3) it reduces the temperature gradient between the melt area and the chamber air to prevent curling (Soe, 2012). It should be noted that during the preheating stage, since the bed temperature

is close to the onset of melting temperature, the unmelted powder may undergo physical and chemical changes after printing (Goodridge et al., 2010; Kuehnlein et al., 2010) and could reduce its reusability. The thermal properties and flowability of the polymer play essential roles in the pre-heating phase (Berretta et al., 2014; Drummer et al., 2010; Tan et al., 2021; Verbelen et al., 2017).

The second phase is laser scanning (B in Fig. 1). Laser scanning of the target area starts once the preheating temperature is stabilized. CO₂ laser (10600 nm wavelength) is the most common laser used in polymer SLS systems because of its high absorptance and low penetration depth in the polymer (Jones, 2013). When the polymer molecular structure interacts with the laser beam, which typically has a size of 500 μm for a CO₂ laser, heat is generated due to the vibration of the polymer's molecular structure. The generated heat raises the temperature above the melting point, but below the T_d , as illustrated by point 2 in Fig. 1. Upon heating, the polymer particles melt, resulting in viscous flow and coalescence. After laser scanning, the molten area rapidly cools down to the printing temperature (point 3 in Fig. 1) (Greiner et al., 2019). Once the layer scanning is completed, the printing bed will move down one layer and a new layer of powder is deposited on the printing bed by a blade or roller. The laser scanning step is repeated until the designed part is fully printed (C in Fig. 1). During the preheating phase as well as the later phases where there is no polymer melting involved, powder deposition is primarily governed by powder–powder interactions (A1 in Fig. 1). During the scanning phase, where there is polymer melt on the top layer, powder deposition is mainly governed by powder–polymer melt interactions (B1 in Fig. 1). Polymer flowability, optical properties, thermal properties, and rheology are the main factors that impact the laser scanning phase (Kruth et al., 2007; Laumer et al., 2016a;

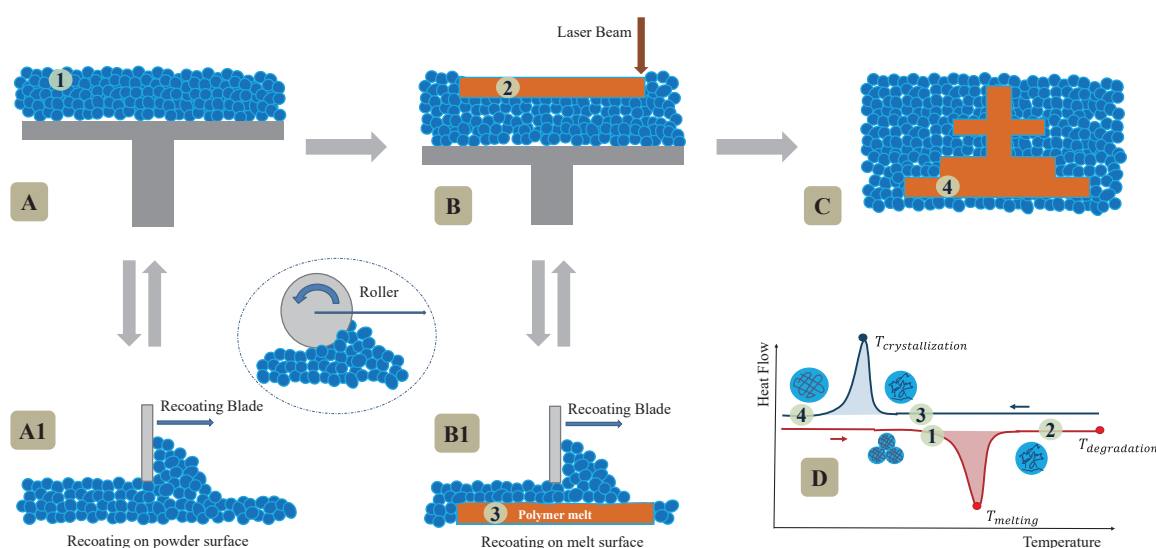


Fig. 1 Polymer SLS process schematic.

Verbelen et al., 2016, 2017; Vock et al., 2019a; Wudy et al., 2015).

After the completion of a printing job, the entire machine, including the printed parts, undergoes a gradual cooling process until it reaches room temperature. The slow cooling process allows the polymer chains to form a crystalline structure (point 4 in Fig. 1). Polymer crystallization plays an essential role in this step (Drummer et al., 2019; Goodridge and Ziegelmeier, 2017; Verbelen et al., 2016).

Fig. 2 illustrates the interplay between operational parameters of the SLS process, particle properties and material properties. Powder properties such as size, shape, size distribution, and surface roughness, not only determine its flowability but also affect the thermal and optical properties of the powder bed (Bierwisch et al., 2021; Myers et al., 2015).

An in-depth understanding of powder flowability is essential for designing a successful SLS material and product development scheme. However, due to the specific spreading mechanism involved in SLS, it is challenging to directly apply existing knowledge from traditional particle science research to SLS systems. The present review aims to provide an overview of the role of powder properties, particle deposition, and flowability characteristics in designing a successful SLS system. Experimental analysis, characterization methods, and computational modeling are reviewed to provide the current state of polymer powder research. Although it is challenging to establish comprehensive quantitative correlations between powder properties, powder deposition, process parameters, and final part properties, the review strives to enhance the understanding

of the factors that influence the SLS powder deposition process and ultimately establish the science-based guidelines for new material development rather than the trial-and-error approaches currently practiced.

2. Flowability overview

In SLS, the powder bed packing density is directly linked to the achievable part density (Schmid et al., 2015). Despite some applications where porous parts are desired (Yan et al., 2017), the main objective of powder deposition in SLS is to transfer the powder from a feed container to the printing bed to form a homogenous and densely packed layer. Therefore, a good flowing powder is a necessary condition to constitute a suitable SLS material. Powder flow properties and flowability are commonly used to evaluate the suitability of a powder for SLS. Additionally, the newly deposited powder layer should exhibit uniform thickness. According to Prescott et al. (2000), powder flow properties are specific bulk characteristics and can be measured. Powder flow properties depend on the particle size distribution, particle shape, surface morphology, density, electrostatic charge, and environmental factors such as temperature and humidity. Powder flowability, on the other hand, refers to the ability of a powder to flow in a desired manner in a specific piece of equipment (Prescott and Barnum, 2000), and depends on powder flow properties, underlying surface layer morphology and spreading (re-coating) mechanism. During recoating on top of the polymer melt scenario, the melt viscosity and surface tension of the molten layer also impact the powder flowability.

From the force perspective, the flowability of SLS powder is influenced by inter-particle forces and external forces

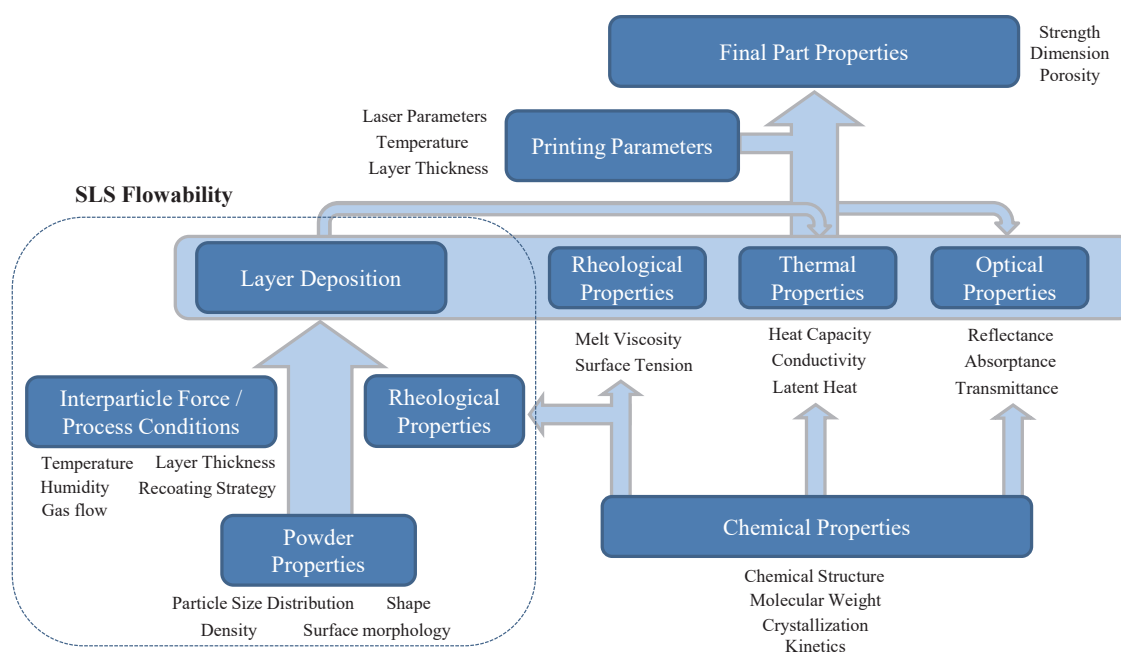


Fig. 2 Graphical representation of the relationships between material properties, printing parameters and final part properties.

due to mechanical interlocking and layer recoating. Van der Waals force, electrostatic force, liquid bridge formation (capillary force), and gravity are the main inter-particle forces between spherical particles (Suzuki, 2019). The van der Waals forces are based on electric dipoles of atoms and molecules. Their magnitude depends on particle size, distance and surface characteristics/morphology (Schulze et al., 2008). Liquid bridge force is formed by the surface tension of the liquid between particles. Considering that the printing temperature of the majority of SLS semi-crystalline polymers is above 100 °C and inert gas is commonly used, the liquid bridge force can be neglected. Electrostatic forces are generated by different electric potentials of particle surfaces (Schulze et al., 2008). Triboelectric charging of polymer powder occurs when the polymer particles come into contact with materials of different dielectric constants (e.g., a metal component) (Tanoue et al., 1999). Due to their low conductivity, it is common practice to allow polymer powder to remain undisturbed for at least 12 hours before printing to reduce/dissipate any electrostatic charge generated during powder preparation. However, triboelectric charging during powder deposition is inevitable. Although the charge build-up between particles improves powder spreading by reducing the attractive van der Waals force and liquid bridge forces, it leads to low packing density (Hesse et al., 2019). Understanding the relationships between these different forces is critical to explaining some of the flowability issues encountered in SLS.



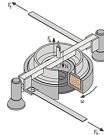
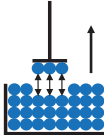
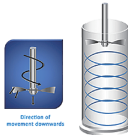
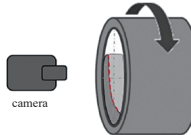

2.1 Flowability characterization

During the material development stage, powder flowability needs to be characterized and optimized before printing. Although the flowability characterization may not represent the powder flow conditions in the SLS process because of the different force and flow mechanisms employed, it can still provide a good indication of the powder flow behavior. Table 1 gives an overview of the flowability characterization methods that have been used in polymer SLS research.

2.2 Flowability measurement techniques

The two most used methods are the angle of repose and Hausner ratio measurement techniques. Although different setups can be used to measure the angle of repose (Schwedes, 2003), the static angle of repose is widely used in SLS (Berretta et al., 2014; Montón Zarazaga et al., 2022; Tan et al., 2017). In the static angle of repose measurements, powder freely flows through a funnel onto a plate. The angle between the developed pile and the plate is defined as angle of repose (Spierings et al., 2016). A small angle of repose represents good flowability. The Hausner ratio is defined as the ratio between the tapped and loose bulk density of the powder. It describes powder compressibility and flowability. Geldart et al. (2006) found a linear relationship between angle of repose and Hausner ratio. Although being widely used in SLS (Arai et al., 2017, 2019; Chatham et al., 2019; Schmid et al., 2013; Wegner, 2021; Ziegelmeier et al., 2015), the Hausner ratio was found to be inaccurate in predicting the flowability of high-density polyethylene composite and polypropylene

Table 1 list of powder flowability characterization methods in polymer SLS.

Methods	Angle of repose (ASTM D6393)	Hausner ratio (ASTM D7481-09) / Carr index (ASTM D6393)	Shear cell (ASTM D6773)	Tensile tester	Powder rheometer (ASTM D7891)	Revolution powder analyzer	Modified film applicator
							
Parameters	<ul style="list-style-type: none"> Angle of repose 	<ul style="list-style-type: none"> Hausner ratio Carr index (C) - loose bulk density - tapped bulk density 	<ul style="list-style-type: none"> Shear force Yield loci 	<ul style="list-style-type: none"> Adhesion force 	<ul style="list-style-type: none"> Basic flowability energy Specific energy Conditioned bulk density 	<ul style="list-style-type: none"> Avalanche angle Surface fractal volume Expansion ratio 	<ul style="list-style-type: none"> Degree of coverage Packing density Packing ratio
References	(Berretta et al., 2014; Montón Zarazaga et al., 2022; Tan et al., 2017)	(Arai et al., 2017, 2019; Chatham et al., 2019; Schmid et al., 2013, 2019; Wegner, 2021; Ziegelmeier et al., 2015)	(Ruggi et al., 2020a, 2020b)	(Schmidt et al., 2014)	(Ziegelmeier et al., 2013, 2015)	(Amado et al., 2011; Amado Becker, 2016; Chatham et al., 2019; Sassaman et al., 2022)	(Laumer et al., 2016b; Van den Eynde et al., 2015; Van den Eynde et al., 2017; Verbelen et al., 2016)

composite materials (Laumer et al., 2016b). Another method that is similar to Hausner ratio but less common in SLS is the Carr index(C) (Schmid et al., 2019), which is the Carr Compressibility as referenced in ASTM D6393 (2021) and can be expressed as,

$$\text{Carr Compressibility} = \frac{\text{Tapped Bulk Density} - \text{Loose Bulk Density}}{\text{Tapped Bulk Density}} \times 100 \quad (1)$$

In addition to the Carr Compressibility, the measurement of Carr Angle of Repose is also described in the ASTM D6393 (2021) to test the flowability and floodability of bulk solids using Carr Indices method.

Tensile strength can also be used to measure SLS powder flowability (Schmidt et al., 2014). This method requires a tensile tester and a smooth loose powder bed. The tensile testing head is coated with jelly. The test starts with the testing head in contact with the powder surface, the first layer of the powder in the container adheres to the jelly-coated testing head. When the powder container moves downward, the force between the stamped powder layer and the remaining powder is measured. The measured force is a combination of gravity and adhesion force between the powder particles. This method provides a good insight into the fundamental interparticle force relationship. However, it is limited in indicating a suitable powder flow behavior.

Shear testers are commonly used to evaluate the powder flowability under well-defined shear conditions. Powder rheological properties like cohesive strength and wall friction under shear can be measured in a shear tester to represent flowability. Ruggi et al. (2020a, 2020b) characterized SLS polymers with a modified high-temperature ring shear tester. Among different types of shear testers, ring shear testers not only provide homogeneous shear displacement (Schulze et al., 2008), but they also have the capability of low normal stress measurements (Vock et al., 2019b). Although the force conditions in ring shear testers are closer to SLS printing conditions compared to other shear testers, the flow mechanism of the shear tester is different from that encountered in SLS (Schmidt et al., 2019). Another characterization method involving shear stress is the powder rheometer. It measures the resistance of a powder to flow against an upward or downward rotating helix under different consolidation conditions. Under specific consolidation and shear conditions, the powder rheometer and shear cell data correlate well with each other (Freeman, 2007).

More recently, the rotational revolution powder analyzer has become more popular (Amado et al., 2011; Amado Becker, 2016; Chatham et al., 2019; Sassaman et al., 2022). It consists of a transparent rotating drum and a camera that records the powder flow conditions in the drum. The Avalanche angle, which is the maximum angle of the powder surface before an avalanche occurs, is considered one

of the most important indices of the rotating powder. The flow of powder in this method is considered closer to SLS process conditions than the other techniques (Spierings et al., 2016). The high temperature measurement capability of this method can provide more insights into powder flow behaviors under SLS temperature conditions (Amado Becker, 2016).

To provide a direct assessment of the powder flowability, some researchers modified a film applicator into a powder spreader with a similar powder spreading mechanism as in SLS (Laumer et al., 2016b; Verbelen et al., 2016; Van den Eynde et al., 2015). A basic powder spreader enables visual observation of the spreading condition. Van den Eynde et al. (2015) set up a powder bed plate on a balance so that layer weight and packing density could be measured in situ to assess powder flowability. Furthermore, a powder spreader with high-temperature capability (up to 140 °C) was developed (Van den Eynde et al., 2017). This modification not only facilitated the characterization of powder for recoating purposes but also allowed for the evaluation of melt surface recoating for low melting temperature polymers.

2.3 Comparative features of various techniques

With the availability of various characterization methods, it is important to understand their relationships, advantages, disadvantages, and differences. Ziegelmeier et al. (2013) compared cohesion, flowability and packing efficiency of polymer powders with different characterization methods—rotational revolution powder analyzer, powder rheometer and the Hausner Ratio technique. Different particle size distributions of a cryogenically ground polyurethane powder and standard PA12 were used to study the effect of both particle size distributions and particle shape. The revolution powder analyzer showed the best reproducible and reliable results under all experimental conditions examined.

Krantz et al. (2009) investigated the relationship between different characterization techniques using two different formulations of powders with particle sizes ranging between 22 to 31 μm. Characterization methods included angle of repose, powder rheometer and revolution powder analyzer. A linear relationship between angle of repose and avalanche angle was discovered regardless of powder formulation. This is because both techniques involve similar force conditions. Additionally, a linear relationship was discovered between angle of repose and cohesion (powder rheometer characterization index) for individual powder types. However, the trend line for different powders did not overlap because of the different forces encountered in the two techniques. The authors concluded that matching the measured and process force conditions is critical for reliable flowability characterization. Furthermore, they emphasized that utilizing multiple characterization techniques

provides a more comprehensive understanding of powder flowability compared to relying on a single technique alone.

The above discussion highlights that each flowability characterization technique focuses on examining powder flowability from a specific perspective related to a particular flow mechanism. The modified film applicator simulates the SLS flow behavior; however, the setup is not easily accessible. Therefore, it is important to obtain a better understanding of powder flowability by applying multiple flowability characterization techniques during the new material development.

3. Role of powder properties

3.1 Particle size distribution (PSD)

To achieve high surface quality and printing accuracy, smaller particle sizes are theoretically preferred. However, for fine powders, van der Waals forces are significantly greater than gravity which causes powder agglomeration issues leading to nonuniformity of layer thickness, and particle packing inhomogeneity during flow (Krantz et al., 2009). While polydisperse powders can benefit particle packing in free flow conditions (McGEARY, 1961), it is often limited by polymer powder production methods. From the laser material interactions perspective, a narrow PSD is preferred to obtain homogeneous melting (Berretta et al., 2014; Wegner, 2021). With the above considerations, a particle size range of 45 to 90 μm is usually preferred (Goodridge and Ziegelmeier, 2017), although some authors have reported this range to be from 20 to 80 μm (Schmid et al., 2015; Vock et al., 2019b).

Beitz et al. (2019) sieved PA12 into three grades: PA12 Coarse ($D_{50} = 56.80 \mu\text{m}$), PA12 Original ($D_{50} = 51.14 \mu\text{m}$) and PA12 Fine ($D_{50} = 46.03 \mu\text{m}$). All grades had an identical level of PSD span, which is defined as $(D_{90} - D_{10})/D_{50}$. The powders were characterized by Hausner ratio and used for laser printing under the same conditions. The three grades of PA12 showed no difference in either flowability or surface roughness of the printed parts. However, it is important to note that this conclusion should be considered valid only within the particle size range examined in this study. A larger difference in D_{50} could lead to different results.

As part of a flowability study by Van den Eynde et al. (2015), standard PA12 powder with a mass-median diameter of 59 μm was compared with a smaller average particle size PA12 (around 42 μm). The PSD span of standard PA12 (0.84) was higher than the smaller PA12 (0.58). A customized powder spreader setup that simulated the SLS spreading process was used to characterize flowability. The smaller PA12 showed lower packing density. Compared to the results from Beitz et al., it is inferred that the span of PSD plays a vital role in flowability; with a similar PA12 particle size in both studies, a smaller span could result in

lower packing density.

It is noteworthy that the effect of PSD span has also been reported in a review primarily focusing on ceramic and metal powders (Vock et al., 2019b). With increasing PSD span, the printed part density and surface quality increased, but the mechanical properties decreased. This indicates that a higher PSD span improves particle packing and part density, however, it can lead to inhomogeneous melting and reduced mechanical properties. However, in a comparison between two commercially available PA12 powders, Schmid et al. (2017) suggested that powder with a smaller span exhibits better flowability and high packing density. Even though the different inter-particle forces could lead to opposite results, more systematic studies are needed to improve the understanding of the flow mechanism during the polymer SLS process.

Multiple studies have been conducted to identify a suitable PSD for SLS. Ziegelmeier et al. (2015) compared the flowability and printability of thermoplastic polyurethane (TPU) and thermoplastic elastomer Duraform Flex (DF). Except for the original particle size fraction, two additional fractions were obtained by sieving out particles below 25 μm or 45 μm . The overall packing density, flowability, printed part surface roughness, ultimate tensile strength and the elongation at break were found to be higher with a decreasing number of fine particles. It was concluded that the gravitational forces increase with particle size, resulting in reduced cohesiveness and improved flowability. Similarly, Schmid et al. (2015) compared two powders with similar volume distribution but different number distribution. The powder with a significant number of small particles (below 20 μm) failed the processability testing due to a higher ratio of cohesion to gravity forces.

On the contrary, other researchers reported the benefits of small particles for powder flow. Verbelen et al. (2016) compared PA6, PA11 and PA12 from different manufacturers with PA11 consisting of rough particles with sharp edges and a large fraction of smaller particles ($D_{10} = 20.6 \mu\text{m}$). Surprisingly, the rough PA11 had a higher packing density. One of the reasons the authors concluded was that the large fraction of smaller particles allowed more efficient packing at the given layer thickness. Although no quantified values were reported, this study along with the previous two studies emphasized that a smaller number of fine particles in the distribution promotes powder flow possibly due to the ball bearing effect, while an excess number of fine particles hinders flow due to agglomeration.

It should be noted that the PSD directly impacts the SLS printing results by changing the powder bed packing density. Indirectly, PSD changes the thermal and optical properties of the powder bed. The powder thermal conductivity is significantly lower than the bulk because of the high porosity of powder beds (Gong et al., 2013). Sillani et al.

reported a positive linear relationship between packing density and thermal conductivity for several SLS polymer powders (Sillani et al., 2021). The porosity also changes powder optical properties which in turn affects the amount of heat energy generated by laser–material interaction. In an infrared spectroscopy study, quantitative infrared directional–hemispherical reflectance spectra were obtained using a commercial integrating sphere (Myers et al., 2015). The results suggested that the optical reflectivity drops with increased particle size for most wavelengths. With a higher optical reflectivity, higher laser energy is needed to compensate for the energy loss. Overall, the change of powder optical reflectivity and thermal conductivity resulting from the PSD should be considered when selecting the laser power and laser scanning rate for a given material.

3.2 The impact of Particle morphology

In free-flowing particle packing, particles with high roundness and low roughness exhibit reduced mechanical interlocking and increased packing density (German, 1989; Hettiarachchi and Mampearachchi, 2020). Thus, particle morphology is important for the SLS process as well (Schmid et al., 2014; Van den Eynde et al., 2015; Verbelen et al., 2016).

In the spreading study conducted by Van den Eynde et al. (2015), medium roundness standard PA12, medium roundness PA12 with smoother edges, high roundness mono-disperse Polystyrene (PS) and low roundness TPU were compared with a customized powder spreader. The high roundness PS exhibited the highest packing density and layer smoothness. Smoother edge PA12 had a higher packing density than the standard PA12. The low roundness TPU had the lowest packing density and resulted in incomplete layers. Accordingly, the high roundness and low roughness were emphasized as the optimal particle morphology conditions for SLS.

However, the high roundness and low roughness particles are not always available for SLS due to the limitation of polymer powder production methods. The current commercially available SLS powder is produced by three main methods: co-extrusion of two non-compatible polymers, precipitation of polymer solutions and cryogenic milling of large polymer granules. Co-extrusion methods produce spherical and smoother particles. However, only limited polymers can be produced by this method, one example is Polypropylene from IRPD AG. The most popular potato shape PA12 powders, such as PA2200 from EOS GmbH, is produced by the precipitation method. Cryogenic milling can process a wide range of polymers by milling below glass transition temperatures. However, milled particles result in irregular shapes and rough surfaces due to the random mechanical force application during the size reduction process. Cryogenic milling also generates a large amount of fine particles which reduces the powder flow-

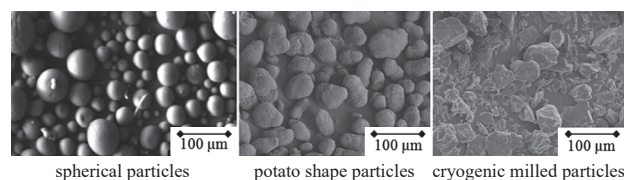


Fig. 3 Typical SLS powder particle shapes (Reprinted with permission from AIP Conference Proceedings “open access”, Schmid et al., 2015).

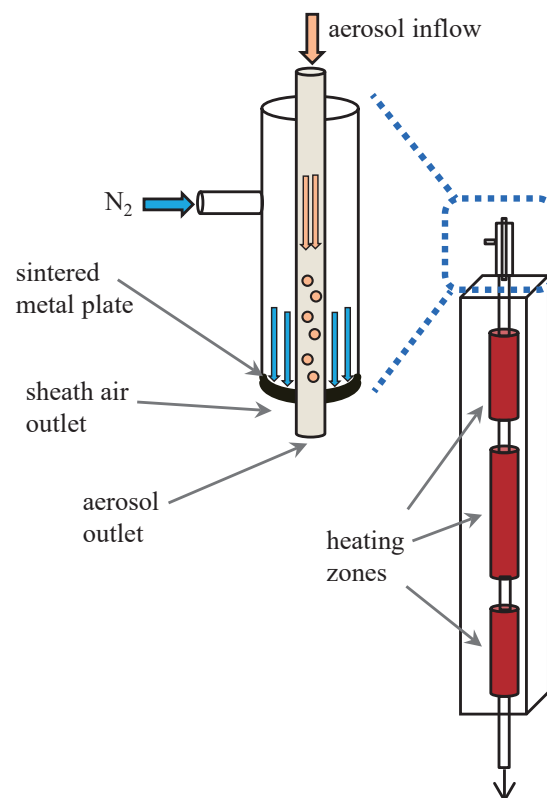


Fig. 4 Schematic drawing of downer reactor (Reprinted with permission from Procedia Engineering “open access”, Sachs et al., 2015).

ability (Schmid et al., 2014). Some typical SLS powder particle shapes are shown in Fig. 3.

In addition to the commercially available methods, multiple techniques have been developed in the literature to improve flowability by generating high-roundness particles.

Berretta et al. (2014) found that virgin PEEK particles did not yield a smooth powder bed during powder deposition. The powder was annealed at a temperature above its glass transition temperature for 24 hours in an air-ventilated oven, left to cool down naturally and sieved. The thermal treatment improved particle roundness and flowability significantly, ultimately enabling a smooth spreading within the printing system.

Downer reactor as shown in Fig. 4, which utilizes the effect of the surface tension of the molten polymer, is commonly used to smooth irregular polymer particles (Sachs et al., 2015). Schmidt et al. (2014; 2016) demonstrated the

rounding process of polystyrene (PS) and polybutylene terephthalate (PBT) powder and introduced a procedure to generate spherical particles for SLS. The polymer micro-particles were produced by wet grinding first. Then the particle roundness was improved by passing them in a heated downer reactor. Finally, hydrophobic fumed silica was mixed with the polymer powder to further improve the flowability by reducing the interparticle van der Waals forces.

4. The impact of processing conditions

During layer deposition, factors such as layer thickness, spreading speed, spreading tool, and temperature are some of the important operational parameters that affect SLS process performance. The impact of these process conditions has also been reported in the literature.

4.1 Layer thickness

For given powder flow characteristics, the desired printing layer thickness depends on different product requirements. A smaller layer thickness is desired to improve printing resolution, but it is limited by the particle size discussed in the previous section. On the other hand, a larger layer thickness reduces printing time. The decreased printing time improves manufacturing efficiency and reduces overall cost. In general, the layer thickness in polymer SLS ranges from 80 to 150 μm . During the deposition of the subsequent layer, melting of the previous layer causes shrinkage in the bed thickness. New powder needs to form a smooth layer on top of the sintered bed. Static and dynamic wall effects are the other main mechanisms of voids formation during the sintering process (Chen et al., 2019). The static wall voids in SLS occur among particles, printing bed and spreading tool due to the round shape of the particles. On the other hand, dynamic wall voids are caused by the arches formed between particles during the spreading motion. In the scenario where particle size and shape cannot be modified to improve packing, increasing the layer thickness can improve the packing density by reducing both the static and dynamic wall effects. Dechet et al. (2020) utilized a layer thickness of 1.5 times the D_{90} , corresponding to around 300 μm , in PLLA development. Although this significantly thicker layer provided promising flowability, it compromised the printing resolution.

4.2 Spreading blade/roller

Blade and roller (counter-rotating with respect to the advancement direction) are the most common powder-spreading tools in SLS systems. The design and movement of the spreading tool also affect the powder packing condition.

Beitz et al. (2019) compared three blade geometries in PA12 printing, including flat, round and sharp bottom. The flat bottom blade shape resulted in the most uniform and

dense powder bed due to the larger horizontal contact zone between the blade and the powder bed.

Haeri et al. (2017) simulated the spreading tool and its speed using discrete element simulation and validated the predicted values with experimental results. The use of a roller produced better bed quality compared to the flat bottom blade because of the adequate contact of a roller, which prevented particle dragging. It was also found that the lower roller translational speed produced better powder bed quality compared to a higher speed. It should be noted that non-spherical (rod-shaped) particles were used in this work which might not represent the spreading conditions of spherical or potato shape particles.

Drummer et al. (2015) investigated the effect of spreading speed with both blade and roller systems. The reproducibility of three spreading speeds (125 mm/s, 250 mm/s, 500 mm/s) was analyzed. An optimal spreading speed of 250 mm/s was found independent of spreading tools. The optimal speed was based on the curling phenomenon due to the temperature gradient after laser scanning as shown in Fig. 5. With a low speed, the long roller and molten area interaction time led to significant cooling of the molten area. Consequently, curling got worse and the warped layer became stuck to the roller and failed to print. With high speed, the varying compression force could shift the slightly curled section and fail the print.

Niino and Sato (2009) proposed a powder compaction method by using a two-steps roller spreading technique as shown in Fig. 6. Compaction was carried out by using a roller of whose rotation speed was controlled independent of its traversing speed. After a traditional roller spreading and layer formation, the powder bed moved up and an additional roller spreading step using the same roller was applied to compact the powder bed. This additional process improved the packing density of the powder bed by a factor of 20 % and reduced residual porosity by 30 %.

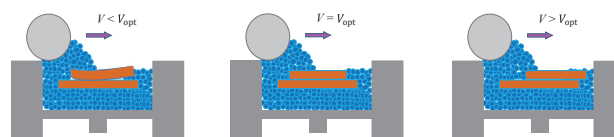


Fig. 5 The effect of powder recoating speed on molten areas.

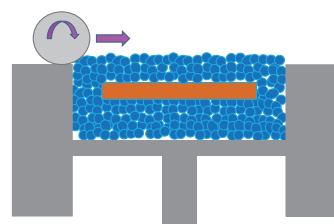


Fig. 6 Powder bed compacting step.

4.3 Other in-process factors

In addition to the powder properties and layer spreading mechanisms, there are other factors in the printing process that also affect powder flowability. One of the most crucial factors is the elevated temperature during the SLS process. The effect of elevated temperature on the flowability is threefold. (1) The polymer particles become softer thereby introducing additional forces by changing contact area and friction between particles during powder flow. (2) Humidity induces cohesive forces between the particles and strongly affects the flow of powders (Rescaglio et al., 2017). For the polymer with a melting temperature above 100 °C, the moisture in the powder evaporates during printing and liquid bridge force gets minimized. Both changes under the elevated temperature cannot be captured with the most powder flowability measurements. (3) The extended long time under elevated temperatures causes changes in the properties of unused powder, which affects its flowability during recycling.

Van den Eynde et al. (2017) examined PA12 flowability under elevated temperatures with a customized powder spreader. A slight increase in the packing condition was observed above the glass transition temperature, indicating that the softening of the polymer increased the powder compressibility. Similarly, Amado et al. (2014) compared PA12 and a co-polypropylene using a modified revolution powder analyzer. The results showed PA12 has reduced surface fractal and improved flowability when process temperatures were above its glass transition temperature.

Ruggi et al. (2020a; 2020b) evaluated PA12 flowability with a high-temperature annular shear cell. The flowability was characterized using the “free-flowing range” method (ASTM D6773). The results showed that the flowability improved from 25 °C to 100 °C, then reduced from 100 °C to 160 °C. The liquid bridges present at 25 °C were proposed as the main limitation of the free flow. The flowability increased with reduced moisture from 25 °C to 100 °C. From 100 °C to 160 °C, powder became cohesive towards close to melting temperature because the softened polymer induced more contact points and contact area which reduced the flowability.

In the earlier discussion of morphology, it was mentioned that PEEK flowability can be optimized by high-temperature annealing. However, high-temperature annealing is not always desired. In a SLS print, most of the powder is not melted. It is important to recycle the unmelted powder to reduce the production cost (Dotchev and Yusoff, 2009). The recycling process involves sieving and storing the unmelted powder, which is then mixed with fresh powder for the next cycle of use. The purpose of powder mixing is to neutralize the changes in the properties of used powder that occur as a result of prolonged exposure to elevated temperatures. The mixing rate depends on the extent of property change in the used powder, and not all the poly-

mers can be recycled (Dadbakhsh et al., 2017; Mwanja et al., 2021). The change in the chemical structure, thermal properties and rheology properties of the used polymer have been well researched in the literature, especially for PA12 (Dooher et al., 2021; Kuehnlein et al., 2010; Wudy et al., 2014). Mielicki et al. (2015) reported a higher PA12 particle shape deviation for particle size bigger than 100 µm and longer aging times. Dadbakhsh et al. (2017) observed an increased cracking in used PA12 from scanning electron microscope images. The cracks might be caused by the evaporation of remaining alcohol and absorbed moisture and/or the subsequent expansion/shrinkage steps of the process cycles. From the powder flowability perspective, Wegner et al. (2014) reported reduced flowability of used polypropylene (PP) based on the Hausner-ratio method. On the contrary, Yang et al. (2021) reported an improved flowability of used PA12 based on the powder rheometer measurement. The discrepancy in flowability results could be attributed to the different measurement methods employed, where the simulated forced flow in a powder rheometer may yield different outcomes compared to free flow and tapped-based Hausner ratio methods.

In our study, both new and used PA12 were evaluated with the Hausner-ratio method. As shown in **Table 2**, new PA12 exhibits a lower Hausner-ratio compared to used PA12, which suggested a reduced flowability of used PA12. The used PA12, on the other hand, has a higher tapped density. Comparing this with the higher flowability in the previously mentioned PA12 powder rheometer measurement results, there could be a similarity between the tapped force during tapped density measurement and the simulated forced flow in the powder rheometer measurement.

Systematic studies of the triboelectric phenomena in polymer SLS are rare. Recently, Hesse et al. (2019) investigated the triboelectric charge of fresh and used PA12. A powder spreading setup with the electrostatic voltmeter was used to compare both fresh and aged PA12. The electrostatic charge build-up of used PA12 was found to be significantly higher than the fresh PA12. The degradation of an antistatic agent in the powder, or the electrical properties change due to the post-condensation were the reasons cited for the observation according to the author. This

Table 2 Hausner ratio of new and used PA12. The raw data on the Hausner ratio is available publicly at <https://doi.org/10.50931/data.kona.23741511>

Material	Loose bulk density (g/cm ³)	Tapped bulk density (g/cm ³)	Hausner ratio
New PA12	0.44	0.51	1.15 ± 0.01
Used PA12	0.42	0.52	1.23 ± 0.02

finding is important for the analysis of powder flowability and the development of powder recycling strategies.

5. Additives

Another approach to improve or modify material flow properties is combining additives with established SLS materials (Arai et al., 2018; Gulotty et al., 2013; Mousah, 2011; Sivadas et al., 2021; Tolochko et al., 2000; Yan et al., 2009; Yuan et al., 2019). Additives, especially hydrophobic fumed silica, have been widely used as flow aids to improve powder flowability (Berretta et al., 2014; Laumer et al., 2013; Schmidt et al., 2014, 2016; Verbelen et al., 2016). The presence of the flow aids reduces the interparticle van der Waals forces (Schmidt et al., 2014) and the effects of electrostatic charges (Lexow and Drummer, 2016).

Considering the significantly small particle size of flow aids, they have a large surface-to-volume ratio, and only a small percentage needs to be added to the polymer matrix. The optimal amount of flow aids is of great interest. Laumer et al. (2016b) investigated the effect of flow aids content in high-density polyethylene (PE-HD, $D_{50} = 57 \mu\text{m}$) and polypropylene (PP, $D_{50} = 100 \mu\text{m}$). Weight concentrations of 0.0 %, 0.1 %, 0.25 % and 1.0 % of nano-scaled fumed silica were mixed with the polymer by dry mixing. The Hausner ratio and degree of coverage were measured to evaluate flowability. The degree of coverage measurement was done by a customized powder spreader. The results showed that the addition of fumed silica improved overall flowability. However, the concentration effect differed between the two characterizations. The Hausner ratio increased with increasing concentration, with 0.1 % as the optimal concentration. On the other hand, in PE-HD degree of coverage testing, saturation was observed at 0.25 % and degree of coverage decreased above this concentration. The proposed explanation was that the increased amount of fumed silica after saturation caused the separation of fumed silica and polymer particles, and/or the fumed silica agglomeration reduced flowability. On the contrary, no satu-

ration was found in the PP system. The degree of coverage continuously increased with the increase in fumed silica amount, which could be attributed to the different particle sizes and inter-particle forces between the two polymers.

Similarly, Kleijnen et al. (2019) reported the effect of fume silica concentration ranging from 0.005 % to 0.5 % in a PBT ($D_{50} = 41.5 \mu\text{m}$) powder system. Hausner ratio and a revolution powder analyzer were used to characterize the flowability. The results showed that the flowability did not change below 0.01 wt%, increased from 0.01 wt% to 0.1 wt%, then reached a plateau. Additionally, SEM images revealed that at 0.5 wt% of additive, the polymer surfaces were fully covered and aggregates were formed, which could justify the flowability plateau.

6. White spot

Besides the lack of a comprehensive understanding of powder flow mechanisms discussed in the previous sections, there are two other major areas that require further investigation.

Most of the existing powder flowability studies were conducted to improve particle packing. However, there are situations where a low packing density can be advantageous, such as when reducing printing time or achieving a porous product is desired. According to Beer-Lambert law, the laser intensity along with the powder depth as it transmits into a media decays exponentially (Osmanlic et al., 2018; Xin et al., 2017). A low particle packing density allows for a slow decay of the laser, which leads to deeper melting depth compared to a high powder packing density bed as shown in Fig. 7. A larger layer thickness can be employed in this condition which reduces the overall printing time. However, there are two potential penalties for printing with a low packing density. First, the high laser scattering caused by low packing density could lead to issues with printed part dimension, such as over-sintering. Second, extremely high melting depth could result in high surface temperatures, potentially leading to polymer

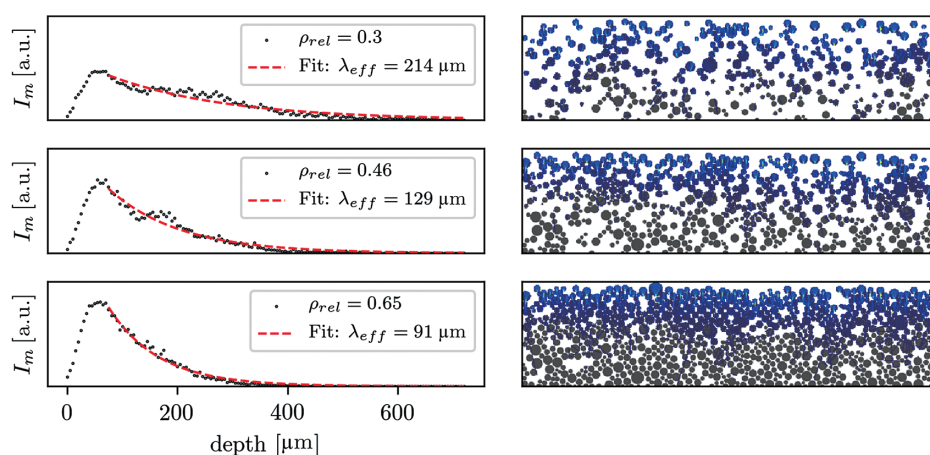


Fig. 7 Laser–powder interaction under different packing densities (Reprinted with permission from Polymers “open access”, Osmanlic et al., 2018).

Table 3 The effect of powder properties and process conditions on SLS–other polymers.

Factors		Optimal range	SLS process			SLS printed part (Caused by flowability change)	Research needs
			Flowability	Layer smooth- ness	Packing density		
Powder property - PSD	+ Span	45 to 90 μm (Goodridge and Ziegelmeier, 2017).			+ (PA12) (Van den Eynde et al., 2015) – (PA12) (Schmid et al., 2017)	– Homogeneous melting [49]	1. Detailed design of experiment to find out the optimal PSD 2. Improved polymer powder production methods
	+ D_{50}	20 to 80 μm (Schmid et al., 2015; Vock et al., 2019b) (General guild line, No experimental data support)	0 (PA12) (Beitz et al., 2019)		+ (PA12) (Van den Eynde et al., 2015)	0 Surface rough- ness (PA12) (Beitz et al., 2019)	
	+ Fine particles		– (TPU, TPE) (Ziegelmeier et al., 2015) – (Schmid et al., 2015)		– (TPU, TPE) (Ziegelmeier et al., 2015) + (PA11, PA12) (Verbelen et al., 2016)	– Tensile strength (TPU, TPE) (Ziegelmeier et al., 2015) – Surface rough- ness (TPU, TPE) (Ziegelmeier et al., 2015) 0 Shore hardness (TPU, TPE) (Ziegelmeier et al., 2015)	
Powder property - Morphol- ogy	+ Roundness	High roundness (Berretta et al., 2014; Haeri et al., 2017; Van den Eynde et al., 2015)	+ (PEEK) (Berretta et al., 2014) + (Haeri et al., 2017)	+ (PA12) (Van den Eynde et al., 2015)	+ (Haeri et al., 2017) + (PA12) (Van den Eynde et al., 2015)		
	+ Roughness	Low roughness (Van den Eynde et al., 2015)			– (PA12) (Van den Eynde et al., 2015)		
Recoating	+ Layer thickness		+ (PLLA) (Dechet et al., 2020) + (HDPE, PP) (Laumer et al., 2016b)				3. Low packing density and large layer thickness scenario
	+ Blade flatness	Flat (Beitz et al., 2019)		+ (PA12) (Beitz et al., 2019)	+ (PA12) (Beitz et al., 2019)		
	+ Roller instead of blade	Roller (Haeri et al., 2017)		+ (Haeri et al., 2017)			4. Powder– polymer melt recoating scenario
	+ Recoating speed	250 mm/s (Drummer et al., 2015)		– (Simulation) (Haeri et al., 2017) +– (PA12) (Drummer et al., 2015)			
Process conditions	+ Temperature		+ (PA12) (Amado et al., 2014) +– (PA12) (Ruggi et al., 2020a, 2020b)	+ (PA12) (Van den Eynde et al., 2017)			5. Aging effect on powder property change in different polymer systems
	+ Reuse	Fresh Powder (Wegner and Ünlü, 2016)	– (PP) (Wegner and Ünlü, 2016) + (PA12) (Yang et al., 2021)				
Particle additives	+ Concentration	0.25 wt% Fumed silica in HDPE, 1 wt.% Fumed silica in PP (Laumer et al., 2016b)		+– (Fumed silica in HDPE, PP) (Laumer et al., 2016b)			
		0.1 wt% Fumed silica in PBT (Kleijnen et al., 2019)		(Fumed silica in PBT) (Kleijnen et al., 2019)			

“+” denotes a positive effect with an increased factor, “–” a negative effect with an increased factor, “0” for no effect. “+–” denotes a positive, then a negative effect with an increased factor. “()” denoted the polymer used in the cited work.

degradation. The detailed impact of packing density, layer thickness and laser parameters on polymer coalescence is not yet well understood and requires further systematic investigations.

Although studies have been conducted on the relationship between powder flow conditions and printed part properties, there remains a significant knowledge gap regarding powder–polymer melt recoating, as shown in Fig. 1 diagram B1. This fundamentally differs from the widely investigated powder flow behavior on flat powder surfaces, which is a significantly different environment than the relatively uneven polymer melt surfaces in real systems. From a powder flowability perspective, most researchers have analyzed the flowability based on a designated single-layer thickness. However, the layer thickness would be different after melting. The powder packing density is about 40–50 % (Van den Eynde et al., 2015). During melting, the powder layer sinks due to the filling of gaps between particles. This phenomenon leads to powder layer height changes for the next powder deposition. In the case of metal SLS, this powder layer height is 4–5 times the designed layer thickness (Wischeropp et al., 2019). The dramatic increase in the layer thickness could change powder flow behavior. Furthermore, Mielicki et al. (2015) discovered that the temperature of the polymer melt, 10 seconds after laser exposure, is close to the printing temperature, indicating that the polymer is in a viscous flow undercooling stage during the next layer powder deposition. Powder deposition on a surface under viscous flow conditions encounters different force conditions compared to deposition on a cooled solid surface. From a polymer rheology perspective, most of the research has focused on the polymer melt coalescence (Haworth et al., 2013; Mielicki et al., 2012), except for a study by Wudy et al. (2015) who investigated the effect of different polymer melt surface tension conditions on the powder bed formation. The opposite scenario, where powder flows on the polymer melt, remains unexplored.

7. Conclusion and future perspectives

Polymer selective laser sintering is a powder-based additive manufacturing technology. In this paper, we have presented a review focusing on one of the most important aspects of SLS: powder flowability. The powder flowability determines layer packing and the final printed part properties. Besides a brief discussion of the powder flowability characterization methods used in polymer SLS, the primary objective of the review was to provide a better understanding of the powder flow mechanism during the printing process. The powder properties such as PSD and particle morphology play important roles in flowability.

The effect of powder properties and process conditions on SLS process performance, based on the literature cited in this review, is summarized in Table 3. Some factors ex-

hibit contradictory effects when viewed from different perspectives., e.g., PSD span improves packing but results in inhomogeneous melting. There is also a delta between the findings for polymer and metal/ceramic regarding the effect of PSD as discussed in the previous section. The current research on polymer SLS is constrained by the limited variety of powder properties options i.e., availability of spherical, and smooth particles with controllable particle sizes. It is essential to improve existing polymer powder production methods and develop new methods so that the desired powder properties criteria for optimal printing conditions can be developed.

As discussed in the above sections, all material properties contribute to a successful SLS print. Regarding the powder properties and flowability:

- A smooth powder layer formation is the precondition of the layer-by-layer process. It is influenced by powder flowability, morphology and process conditions. The use of an optimal PSD (45–90 μm or 20–80 μm), high roundness particles or an appropriate concentration of flow aids often leads to an acceptable layer formation.
- The powder packing density is influenced by the same factors as powder flowability and can be improved by utilizing an appropriate PSD, high roundness particles and an optimal concentration of flow aids. The packing density affects the thermal and optical properties of the powder bed, which cause a direct impact on the laser–material interaction as shown in Fig. 7. By tuning laser parameters, process conditions and adding absorption intensifiers (Laumer et al., 2013), successful print properties can be achieved even with powder beds that have low packing densities.

In addition to experimental studies, simulations and modeling efforts are needed to provide further insights to develop meaningful guidelines for achieving optimal powder properties and successful process performance.

Considering that PA and its composites account for 95 % of the SLS polymer commercial market, there is a need to develop other polymers to meet diverse product property requirements and expand the range of SLS applications. The current understanding of polymer processing phenomena, including flowability, is primarily based on PA12. As a common approach, investigating the printing mechanism of PA12 and using it as a basis for developing guidelines for new materials is often employed. Without the development of universally quantified criteria for powder/material properties, the trial-and-error method will continue to be the most common approach for new material development in the industry. It is also critical to expand the investigation of other polymers, from feasibility tests to fundamental failure mode analysis, to gain a deeper understanding of the SLS process.

Data Availability Statement

The raw data on Polyamide 12 Hausner ratio is available publicly in J-STAGE Data (<https://doi.org/10.50931/data.kona.23741511>).

Acknowledgments

The authors acknowledge the financial support of the National Science Foundation Center of Particulate and Surfactant Science (CPaSS) and the industry members (NSF Award #1362060). Any opinions, findings, and conclusions or recommendations expressed in this material are those of the authors and do not necessarily reflect the views of the National Science Foundation or the CPaSS industry members.

References

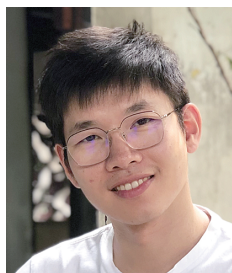
- Amado A., Schmid M., Levy G., Wegener K., Advances in SLS powder characterization, 22nd Annual International Solid Freeform Fabrication Symposium, (2011) 438–452. DOI: 10.26153/tsw/15306
- Amado A., Schmid M., Wegener K., Flowability of SLS powders at elevated temperature, Swiss Institute of Technology, ETH Zürich, 2014. DOI: 10.3929/ethz-a-010057815
- Amado Becker A.F., Characterization and prediction of SLS processability of polymer powders with respect to powder flow and part warpage, Doctoral Thesis, ETH-Zürich, 2016. DOI: 10.3929/ethz-a-010657585
- Arai S., Tsunoda S., Kawamura R., Kuboyama K., Ougizawa T., Comparison of crystallization characteristics and mechanical properties of poly(butylene terephthalate) processed by laser sintering and injection molding, *Materials & Design*, 113 (2017) 214–222. DOI: 10.1016/j.matdes.2016.10.028
- Arai S., Tsunoda S., Yamaguchi A., Ougizawa T., Effects of short-glass-fiber content on material and part properties of poly(butylene terephthalate) processed by selective laser sintering, *Additive Manufacturing*, 21 (2018) 683–693. DOI: 10.1016/j.addma.2018.04.019
- Arai S., Tsunoda S., Yamaguchi A., Ougizawa T., Characterization of flame-retardant poly(butylene terephthalate) processed by laser sintering, *Optics & Laser Technology*, 117 (2019) 94–104. DOI: 10.1016/j.optlastec.2019.04.006
- ASTM D6393, Standard Test Method for Bulk Solids Characterization by Carr Indices, ASTM International, 2021. DOI: 10.1520/d6393_d6393m-21
- Beitz S., Uerlich R., Bokelmann T., Diener A., Vietor T., Kwade A., Influence of powder deposition on powder bed and specimen properties, *Materials*, 12 (2019) 297. DOI: 10.3390/ma12020297
- Benedetti L., Brulé B., Decreamer N., Evans K.E., Ghita O., Shrinkage behaviour of semi-crystalline polymers in laser sintering: PEKK and PA12, *Materials & Design*, 181 (2019) 107906. DOI: 10.1016/j.matdes.2019.107906
- Berretta S., Evans K.E., Ghita O.R., Predicting processing parameters in high temperature laser sintering (HT-LS) from powder properties, *Materials and Design*, 105 (2016) 301–314. DOI: 10.1016/j.matdes.2016.04.097
- Berretta S., Ghita O., Evans K.E., Morphology of polymeric powders in Laser Sintering (LS): from Polyamide to new PEEK powders, *European Polymer Journal*, 59 (2014) 218–229. DOI: 10.1016/j.eurpolymj.2014.08.004
- Bierwisch C., Mohseni-Mofidi S., Dietemann B., Grünewald M., Rudloff J., Lang M., Universal process diagrams for laser sintering of polymers, *Materials & Design*, 199 (2021) 109432. DOI: 10.1016/j.matdes.2020.109432
- Chatham C.A., Long T.E., Williams C.B., Powder bed fusion of poly(phenylene sulfide) at bed temperatures significantly below melting, *Additive Manufacturing*, 28 (2019) 506–516. DOI: 10.1016/j.addma.2019.05.025
- Chen H., Wei Q., Zhang Y., Chen F., Shi Y., Yan W., Powder-spreading mechanisms in powder-bed-based additive manufacturing: experiments and computational modeling, *Acta Materialia*, 179 (2019) 158–171. DOI: 10.1016/j.actamat.2019.08.030
- Dadbakhsh S., Verbelen L., Vandeputte T., Strobbe D., Van Puyvelde P., Kruth J.P., Effect of powder size and shape on the SLS processability and mechanical properties of a TPU elastomer, *Physics Procedia*, 83 (2016) 971–980. DOI: 10.1016/j.phpro.2016.08.102
- Dadbakhsh S., Verbelen L., Verkinderen O., Strobbe D., Effect of PA12 powder reuse on coalescence behaviour and microstructure of SLS parts, *European Polymer Journal*, 92 (2017) 250–262. DOI: 10.1016/j.eurpolymj.2017.05.014
- Dechet M.A., Demina A., Römling L., Gómez Bonilla J.S., Lanyi F.J., Schubert D.W., Bück A., Peukert W., Schmidt J., Development of poly(L-lactide) (PLLA) microspheres precipitated from triacetin for application in powder bed fusion of polymers, *Additive Manufacturing*, 32 (2020) 100966. DOI: 10.1016/j.addma.2019.100966
- Dooher T., Archer E., Walls T., McIlhagger A., Dixon D., Ageing of laser sintered glass-filled Polyamide 12 (PA12) parts at elevated temperature and humidity, *Polymers and Polymer Composites*, 12 (2021) 1–11. DOI: 10.1177/09673911211027127
- Dotchev K., Yusoff W., Recycling of polyamide 12 based powders in the laser sintering process, *Rapid Prototyping Journal*, 15 (2009) 192–203. DOI: 10.1108/13552540910960299
- Drummer D., Drexler M., Wudy K., Density of laser molten polymer parts as function of powder coating process during additive manufacturing, *Procedia Engineering*, 102 (2015) 1908–1917. DOI: 10.1016/j.proeng.2015.01.331
- Drummer D., Greiner S., Zhao M., Wudy K., A novel approach for understanding laser sintering of polymers, *Additive Manufacturing*, 27 (2019) 379–388. DOI: 10.1016/j.addma.2019.03.012
- Drummer D., Rietzel D., Kühnlein F., Development of a characterization approach for the sintering behavior of new thermoplastics for selective laser sintering, *Physics Procedia*, 5 (2010) 533–542. DOI: 10.1016/j.phpro.2010.08.081
- Freeman R., Measuring the flow properties of consolidated, conditioned and aerated powders—a comparative study using a powder rheometer and a rotational shear cell, *Powder Technology*, 174 (2007) 25–33. DOI: 10.1016/j.powtec.2006.10.016
- Geldart D., Abdullah E.C., Hassanpour A., Nwoke L.C., Wouters I., Characterization of powder flowability using measurement of angle of repose, *China Particuology*, 4 (2006) 104–107. DOI: 10.1016/s1672-2515(07)60247-4
- German R.M., Particle Packing Characteristics, Metal Powder Industry, 1989, ISBN: 9780918404831. DOI: 10.1016/0032-5910(90)80071-6
- Gong X., Cheng B., Price S., Chou K., Powder-bed electron-beam-melting additive manufacturing: powder characterization, process simulation and metrology, ASME District Early Career Technical Conference, ASME Early Career Technical Journal, (2013) 59–66.
- Goodridge R., Ziegelmeier S., Powder bed fusion of polymers, *Laser Additive Manufacturing: Materials, Design, Technologies, and Applications*, (2017) 181–204. DOI: 10.1016/B978-0-08-100433-3.00007-5
- Goodridge R.D., Hague R.J.M., Tuck C.J., Effect of long-term ageing on the tensile properties of a polyamide 12 laser sintering material, *Polymer Testing*, 29 (2010) 483–493. DOI: 10.1016/j.polymertesting.2010.02.009
- Greiner S., Wudy K., Wörz A., Drummer D., Thermographic investigation of laser-induced temperature fields in selective laser beam melting of polymers, *Optics and Laser Technology*, 109 (2019) 569–576. DOI: 10.1016/j.optlastec.2018.08.010

- Gulotty R., Castellino M., Jagdale P., Tagliaferro A., Balandin A.A., Effects of functionalization on thermal properties of single-wall and multi-wall carbon nanotube-polymer nanocomposites, *ACS Nano*, 7 (2013) 5114–5121. DOI: 10.1021/nn400726g
- Haeri S., Wang Y., Ghita O., Sun J., Discrete element simulation and experimental study of powder spreading process in additive manufacturing, *Powder Technology*, 306 (2017) 45–54. DOI: 10.1016/j.powtec.2016.11.002
- Haworth B., Hopkinson N., Hitt D., Zhong X., Shear viscosity measurements on Polyamide-12 polymers for laser sintering, *Rapid Prototyping Journal*, 19 (2013) 28–36. DOI: 10.1108/13552541311292709
- Hesse N., Dechet M.A., Bonilla J.S.G., Lübbert C., Roth S., Bück A., Schmidt J., Peukert W., Analysis of tribo-charging during powder spreading in selective laser sintering: assessment of polyamide 12 powder ageing effects on charging behavior, *Polymers*, 11 (2019) 609. DOI: 10.3390/polym11040609
- Hettiarachchi C., Mamppearachchi W.K., Effect of surface texture, size ratio and large particle volume fraction on packing density of binary spherical mixtures, *Granular Matter*, 22 (2020) 1–13. DOI: 10.1007/s10035-019-0978-3
- ISO/ASTM 52900:2021, Additive manufacturing—General principles—Fundamentals and vocabulary, 2021. <<https://www.iso.org/standard/74514.html>> accessed 20042023
- Ituarte I.F., Wiikinkoski O., Jansson A., Additive manufacturing of polypropylene: a screening design of experiment using laser-based powder bed fusion, *Polymers*, 10 (2018) 1293. DOI: 10.3390/polym10121293
- Jones I., Laser welding of plastics, in: Katayama S. (Ed.) *Handbook of Laser Welding Technologies*, Woodhead Publishing, 2013, pp. 280–301e, ISBN: 9780857092649. DOI: 10.1533/9780857098771.2.280
- Kleijnen R.G., Schmid M., Wegener K., Nucleation and impact modification of polypropylene laser sintered parts, *AIP Conference Proceedings*, 1779 (2016) 100004–1–5. DOI: 10.1063/1.4965572
- Kleijnen R.G., Schmid M., Wegener K., Impact of flow aid on the flowability and coalescence of polymer laser sintering powder, 2019 International Solid Freeform Fabrication Symposium, (2019) 806–817. DOI: 10.26153/tsw/17317
- Kleijnen R.G., Sessege J.P.W., Schmid M., Wegener K., Insights into the development of a short-fiber reinforced polypropylene for laser sintering, *AIP Conference Proceedings*, 1914 (2017) 190002. DOI: 10.1063/1.5016791
- Krantz M., Zhang H., Zhu J., Characterization of powder flow: static and dynamic testing, *Powder Technology*, 194 (2009) 239–245. DOI: 10.1016/j.powtec.2009.05.001
- Kruth J.P., Leu M.C., Nakagawa T., Progress in additive manufacturing and rapid prototyping, *CIRP Annals—Manufacturing Technology*, 47 (1998) 525–540. DOI: 10.1016/s0007-8506(07)63240-5
- Kruth J.P., Levy G., Klocke F., Childs T.H.C., Consolidation phenomena in laser and powder-bed based layered manufacturing, *CIRP Annals—Manufacturing Technology*, 56 (2007) 730–759. DOI: 10.1016/j.cirp.2007.10.004
- Kuehnlein F., Drummer D., Rietzel D., Seefried A., Degradation behavior and material properties of PA12-plastic powders processed by powder based additive manufacturing technologies, *Annals of DAAAM and Proceedings of the International DAAAM Symposium*, 21 (2010) 1547–1548. ISBN 9783901509735.
- Laumer T., Stichel T., Nagulin K., Schmidt M., Optical analysis of polymer powder materials for Selective Laser Sintering, *Polymer Testing*, 56 (2016a) 207–213. DOI: 10.1016/j.polymertesting.2016.10.010
- Laumer T., Stichel T., Rath M., Schmidt M., Analysis of the influence of different flowability on part characteristics regarding the simultaneous laser beam melting of polymers, *Physics Procedia*, 83 (2016b) 937–946. DOI: 10.1016/j.phpro.2016.08.098
- Laumer T., Stichel T., Sachs M., Amend P., Schmidt M., Qualification and modification of new polymer powders for laser beam melting using Ulbricht spheres, in: *High Value Manufacturing: Advanced Research in Virtual and Rapid Prototyping*, 1st ed., CRC Press, 2013, pp. 255–260. ISBN: 9781138001374. DOI: 10.1201/b15961
- Lexow M.M., Drummer D., New materials for SLS: the use of antistatic and flow agents, *Journal of Powder Technology*, 2016 (2016) 4101089. DOI: 10.1155/2016/4101089
- Ligon S.C., Liska R., Stampfl J., Gurr M., Mülhaupt R., Polymers for 3D printing and customized additive manufacturing, *Chemical Reviews*, 117 (2017) 10212–10290. DOI: 10.1021/acs.chemrev.7b00074
- Lupone F., Padovano E., Casamento F., Badini C., Process phenomena and material properties in selective laser sintering of polymers: a review, *Materials*, 15 (2021) 183. DOI: 10.3390/ma15010183
- McGeary R.K., Mechanical packing of spherical particles, *Journal of the American Ceramic Society*, 44 (1961) 513–522. DOI: 10.1111/j.1151-2916.1961.tb13716.x
- Mielicki C., Gronhoff B., Wortberg J., Effects of laser sintering processing time and temperature on changes in polyamide 12 powder particle size, shape and distribution, *AIP Conference Proceedings*, 1593 (2015) 728–731. DOI: 10.1063/1.4873880
- Mielicki C., Wegner a, Gronhoff B., Wortberg J., Witt G., Prediction of PA12 melt viscosity in laser sintering by a time and temperature dependent rheological model, *RTeJournal*, 32 (2012). <https://rtejournal.de/document/2012_11> accessed 20012023.
- Montón Zarazaga A., Abdelmoula M., Küçüktürk G., Maury F., Ferrato M., Grossin D., Process parameters investigation for direct powder bed selective laser processing of silicon carbide parts, *Progress in Additive Manufacturing*, 7 (2022) 1307–1322. DOI: 10.1007/s40964-022-00305-7
- Mousah A., Effects of filler content and coupling agents on the mechanical properties and geometrical accuracy of selective laser sintered parts in glass bead-filled polyamide 12 composites, Thesis (Ph.D.), Cardiff University, 2011, pp. 227–231. <https://orca.cardiff.ac.uk/id/eprint/11094>
- Mwania F.M., Maringa M., Van Der Walt J.G., A review of the techniques used to characterize laser sintering of polymeric powders for use and re-use in additive manufacturing, *Manufacturing Review*, 8 (2021) 1–17. DOI: 10.1051/mfreview/2021012
- Myers T.L., Brauer C.S., Su Y.-F., Blake T.A., Tonkyn R.G., Ertel A.B., Johnson T.J., Richardson R.L., Quantitative reflectance spectra of solid powders as a function of particle size, *Applied Optics*, 54 (2015) 4863. DOI: 10.1364/ao.54.004863
- Niino T., Sato K., Effect of powder compaction in plastic laser sintering fabrication, 2009 International Solid Freeform Fabrication Symposium, (2009) 193–205. DOI: 10.26153/tsw/15100
- Osmanlic F., Wudy K., Laumer T., Schmidt M., Drummer D., Körner C., Modeling of laser beam absorption in a polymer powder bed, *Polymers*, 10 (2018) 1–11. DOI: 10.3390/polym10070784
- Prescott J., Barnum R.A., On powder flowability, *Pharmaceutical Technology*, 24(10) (2000) 60–84.
- Rescaglio A., Schockmel J., Vandewalle N., Lumay G., Combined effect of moisture and electrostatic charges on powder flow, *EPJ Web of Conferences*, 140 (2017) 13009. DOI: 10.1051/epjconf/201714013009
- Ruggi D., Barrès C., Charneau J.Y., Fulchiron R., Barletta D., Poletto M., A quantitative approach to assess high temperature flow properties of a PA 12 powder for laser sintering, *Additive Manufacturing*, 33 (2020a) 101143. DOI: 10.1016/j.addma.2020.101143
- Ruggi D., Lupo M., Sofia D., Barrès C., Barletta D., Poletto M., Flow properties of polymeric powders for selective laser sintering, *Powder Technology*, 370 (2020b) 288–297. DOI: 10.1016/j.powtec.2020.05.069
- Sachs M., Schmidt J., Toni F., Blümel C., Winzer B., Peukert W., Wirth K.E., Rounding of irregular polymer particles in a downer reactor, *Procedia Engineering*, 102 (2015) 542–549. DOI: 10.1016/j.proeng.2015.01.119

- Sassaman D., Phillips T., Milroy C., Ide M., Beaman J., A method for predicting powder flowability for selective laser sintering, *JOM*, 74 (2022) 1102–1110. DOI: 10.1007/s11837-021-05050-w
- Schmid M., Amado F., Levy G., Wegener K., Flowability of powders for selective laser sintering (SLS) investigated by round robin test, in: *High Value Manufacturing: Advanced Research in Virtual and Rapid Prototyping*, 1st ed., CRC Press, 2013, pp. 95–99, ISBN: 9781138001374. DOI: 10.3929/ethz-a-010057806
- Schmid M., Amado A., Wegener K., Materials perspective of polymers for additive manufacturing with selective laser sintering, *Journal of Materials Research*, 29 (2014) 1824–1832. DOI: 10.1557/jmr.2014.138
- Schmid M., Amado A., Wegener K., Polymer powders for selective laser sintering (SLS), *AIP Conference Proceedings*, 1664 (2015) 160009–1–5. DOI: 10.1063/1.4918516
- Schmid M., Kleijn R., Vetterli M., Wegener K., Influence of the origin of polyamide 12 powder on the laser sintering process and laser sintered parts, *Applied Sciences (Switzerland)*, 7 (2017) 462. DOI: 10.3390/app7050462
- Schmidt J., Dechet M.A., Gómez Bonilla J.S., Hesse N., Bück A., Peukert W., Characterization of polymer powders for selective laser sintering, 2019 International Solid Freeform Fabrication Symposium, (2019) 779–789. DOI: 10.26153/tsw/17314
- Schmidt J., Sachs M., Blümel C., Winzer B., Toni F., Wirth K.E., Peukert W., A novel process route for the production of spherical LBM polymer powders with small size and good flowability, *Powder Technology*, 261 (2014) 78–86. DOI: 10.1016/j.powtec.2014.04.003
- Schmidt J., Sachs M., Fanselow S., Zhao M., Romeis S., Drummer D., Wirth K.E., Peukert W., Optimized polybutylene terephthalate powders for selective laser beam melting, *Chemical Engineering Science*, 156 (2016) 1–10. DOI: 10.1016/j.ces.2016.09.009
- Schulze D., *Powders and Bulk Solids: Behavior, Characterization, Storage and Flow*, 1st ed., Springer Berlin, Heidelberg, 2008, ISSN: 9783540737674. DOI: 10.1007/978-3-540-73768-1
- Schwedes J., Review on testers for measuring flow properties of bulk solids, *Granular Matter*, 5 (2003) 1–43. DOI: 10.1007/s10035-002-0124-4
- Sillani F., de Gasparo F., Schmid M., Wegener K., Influence of packing density and fillers on thermal conductivity of polymer powders for additive manufacturing, *International Journal of Advanced Manufacturing Technology*, 117 (2021) 2049–2058. DOI: 10.1007/s00170-021-07117-z
- Sivadas B.O., Ashcroft I., Khlobystov A.N., Goodridge R.D., Laser sintering of polymer nanocomposites, *Advanced Industrial and Engineering Polymer Research*, 4 (2021) 277–300. DOI: 10.1016/j.aiepr.2021.07.003
- Soe S.P., Quantitative analysis on SLS part curling using EOS P700 machine, *Journal of Materials Processing Technology*, 212 (2012) 2433–2442. DOI: 10.1016/j.jmatprotec.2012.06.012
- Spierings A.B., Voegtlin M., Bauer T., Wegener K., Powder flowability characterisation methodology for powder-bed-based metal additive manufacturing, *Progress in Additive Manufacturing*, 1 (2016) 9–20. DOI: 10.1007/s40964-015-0001-4
- Stansbury J.W., Idacavage M.J., 3D printing with polymers: challenges among expanding options and opportunities, *Dental Materials*, 32 (2016) 54–64. DOI: 10.1016/j.dental.2015.09.018
- Starr T.L., Gornet T.J., Usher J.S., The effect of process conditions on mechanical properties of laser-sintered nylon, *Rapid Prototyping Journal*, 17 (2011) 418–423. DOI: 10.1108/13552541111184143
- Suzuki M., Chapter 3.5: Packing properties, in: Higashitani K., Makino, H., and Matsusaka, S. (Eds.), *Powder Technology Handbook*, 4th ed., CRC Press, 2019, pp.203–209, ISBN: 9781315184258. DOI: 10.1201/b22268
- Tan L.J., Zhu W., Sagar K., Zhou K., Comparative study on the selective laser sintering of polypropylene homopolymer and copolymer: processability, crystallization kinetics, crystal phases and mechanical properties, *Additive Manufacturing*, 37 (2021) 101610. DOI: 10.1016/j.addma.2020.101610
- Tan Y.-Q., Zheng J.-H., Gao W., Jiang S.-Q., Feng Yuntian, Zheng J., Gao A.W., Jiang A.S., Feng Y., The effect of powder flowability in the selective laser sintering process, *Proceedings of the 7th International Conference on Discrete Element Methods*, 188 (2017) 629–636. DOI: 10.1007/978-981-10-1926-5_65
- Tanoue K.I., Ema A., Masuda H., Effect of material transfer and work hardening of metal surface on the current generated by impact of particles, *Journal of Chemical Engineering of Japan*, 32 (1999) 544–548. DOI: 10.1252/jcej.32.544
- Tolochko N.K., Laoui T., Khlopkov Y.V., Mozharov S.E., Titov V.I., Ignatiev M.B., Absorptance of powder materials suitable for laser sintering, *Rapid Prototyping Journal*, 6 (2000) 155–160. DOI: 10.1108/13552540010337029
- Van den Eynde M., Verbelen L., Van Puyvelde P., Assessing polymer powder flow for the application of laser sintering, *Powder Technology*, 286 (2015) 151–155. DOI: 10.1016/j.powtec.2015.08.004
- Van den Eynde M., Verbelen L., Van Puyvelde P., Influence of temperature on the flowability of polymer powders in laser sintering, *AIP Conference Proceedings*, 1914 (2017) 190007–1–5. DOI: 10.1063/1.5016796
- Vasquez G.M., Majewski C.E., Haworth B., Hopkinson N., A targeted material selection process for polymers in laser sintering, *Additive Manufacturing*, 1 (2014) 127–138. DOI: 10.1016/j.addma.2014.09.003
- Vasquez M., Haworth B., Hopkinson N., Optimum sintering region for laser sintered Nylon-12, *Proceedings of the Institution of Mechanical Engineers, Part B: Journal of Engineering Manufacture*, 225 (2011) 2240–2248. DOI: 10.1177/0954405411414994
- Verbelen L., Dadbakhsh S., Van den Eynde M., Kruth J.P., Goderis B., Van Puyvelde P., Characterization of polyamide powders for determination of laser sintering processability, *European Polymer Journal*, 75 (2016) 163–174. DOI: 10.1016/j.eurpolymj.2015.12.014
- Verbelen L., Dadbakhsh S., Van den Eynde M., Strobbe D., Kruth J.P., Goderis B., Van Puyvelde P., Analysis of the material properties involved in laser sintering of thermoplastic polyurethane, *Additive Manufacturing*, 15 (2017) 12–19. DOI: 10.1016/j.addma.2017.03.001
- Vock S., Klöden B., Kirchner A., Weißgärber T., Kieback B., Powders for powder bed fusion: a review, *Progress in Additive Manufacturing*, 4 (2019a) 383–397. DOI: 10.1007/s40964-019-00078-6
- Vock S., Klöden B., Kirchner A., Weißgärber T., Kieback B., Powders for powder bed fusion: a review, *Progress in Additive Manufacturing*, 4 (2019b) 383–397. DOI: 10.1007/s40964-019-00078-6
- Wegner A., New polymer materials for the laser sintering process: polypropylene and others, *Physics Procedia*, 83 (2016) 1003–1012. DOI: 10.1016/j.phpro.2016.08.105
- Wegner A., Introduction to powder bed fusion of polymers, *Additive Manufacturing*, (2021) 33–75. DOI: 10.1016/B978-0-12-818411-0.00011-2
- Wegner A., Mielicki C., Grimm T., Gronhoff B., Witt G., Wortberg J., Determination of robust material qualities and processing conditions for laser sintering of polyamide 12, *Polymer Engineering and Science*, 54 (2014) 1540–1554. DOI: 10.1002/pen.23696
- Wegner A., Ünlü T., Powder life cycle analyses for a new polypropylene laser sintering material, 2016 International Solid Freeform Fabrication Symposium, (2016) 834–846. <https://hdl.handle.net/2152/89636>
- Williams J.M., Adewunmi A., Schek R.M., Flanagan C.L., Krebsbach P.H., Feinberg S.E., Hollister S.J., Das S., Bone tissue engineering using polycaprolactone scaffolds fabricated via selective laser sintering, *Biomaterials*, 26 (2005) 4817–4827. DOI: 10.1016/j.biomaterials.2004.11.057
- Wischeropp T.M., Emmelmann C., Brandt M., Pateras A., Measurement of actual powder layer height and packing density in a single layer in

- selective laser melting, *Additive Manufacturing*, 28 (2019) 176–183. DOI: 10.1016/j.addma.2019.04.019
- Wudy K., Drummer D., Drexler M., Characterization of polymer materials and powders for selective laser melting, *AIP Conference Proceedings*, 1593 (2015) 702–707. DOI: 10.1063/1.4873875
- Wudy K., Drummer D., Kühnlein F., Drexler M., Influence of degradation behavior of polyamide 12 powders in laser sintering process on produced parts, *AIP Conference Proceedings*, 1593 (2014) 691–695. DOI: 10.1063/1.4873873
- Xin L., Boutaous M., Xin S., Siginer D.A., Multiphysical modeling of the heating phase in the polymer powder bed fusion process, *Additive Manufacturing*, 18 (2017) 121–135. DOI: 10.1016/j.addma.2017.10.006
- Yan C., Shi Y., Hao L., Investigation into the differences in the selective laser sintering between amorphous and semi-crystalline polymers, *International Polymer Processing*, 26 (2011) 416–423. DOI: 10.3139/217.2452
- Yan C.Z., Shi Y.S., Yang J.S., Xu L., Preparation and selective laser sintering of nylon-12-coated aluminum powders, *Journal of Composite Materials*, 43 (2009) 1835–1851. DOI: 10.1177/0021998309340932
- Yan M., Tian X., Peng G., Cao Y., Li D., Hierarchically porous materials prepared by selective laser sintering, *Materials and Design*, 135 (2017) 62–68. DOI: 10.1016/j.matdes.2017.09.015
- Yang F., Schnuerch A., Chen X., Quantitative influences of successive reuse on thermal decomposition, molecular evolution, and elemental composition of polyamide 12 residues in selective laser sintering, *International Journal of Advanced Manufacturing Technology*, 115 (2021) 3121–3138. DOI: 10.1007/S00170-021-07368-W/TABLES/7
- Yuan S., Shen F., Bai J., Chua C.K., Wei J., Zhou K., 3D soft auxetic lattice structures fabricated by selective laser sintering: TPU powder evaluation and process optimization, *Materials & Design*, 120 (2017) 317–327. DOI: 10.1016/J.MATDES.2017.01.098
- Yuan S., Shen F., Chua C.K., Zhou K., Polymeric composites for powder-based additive manufacturing: materials and applications, *Progress in Polymer Science*, 91 (2019) 141–168. DOI: 10.1016/j.progpolymsci.2018.11.001
- Zhu W., Yan C., Shi Yunsong, Wen S., Han C., Cai C., Liu J., Shi Yusheng, Study on the selective laser sintering of a low-isotacticity polypropylene powder, *Rapid Prototyping Journal*, 22 (2016) 621–629. DOI: 10.1108/RPJ-02-2015-0014
- Ziegelmeier S., Christou P., Wöllecke F., Tuck C., Goodridge R., Hague R., Krampe E., Wintermantel E., An experimental study into the effects of bulk and flow behaviour of laser sintering polymer powders on resulting part properties, *Journal of Materials Processing Technology*, 215 (2015) 239–250. DOI: 10.1016/j.jmatprotec.2014.07.029
- Ziegelmeier S., Wöllecke F., Tuck C., Goodridge R., Hague R., Characterizing the bulk & flow behaviour of ls polymer powders, *Solid Freeform Fabrication Symposium*, (2013) 354–367. DOI: 10.26153/tsw/15437

Authors' Short Biographies



Xi Guo

Xi Guo received his bachelor's degree in process equipment and control engineering from the Beijing University of Chemical Technology in 2014. He went to graduate school at the University of Florida and received his master's degree in mechanical engineering in 2016. Afterward, he worked for Johnson and Johnson as a materials engineer. In 2022, he completed his doctoral degree under the advisement of Dr. Brij M. Moudgil, Department of Materials Science and Engineering, University of Florida. His current research focus is on polymer selective laser sintering.



Brij M. Moudgil

Dr. Brij M. Moudgil is a Distinguished Professor of Materials Science and Engineering at the University of Florida. He received his B.E from the Indian Institute of Science, Bangalore, India, and his M.S. and Eng.Sc.D. degrees from Columbia University, New York. His current research interests are in surfactant and polymer adsorption, dispersion and aggregation of fine particles, adhesion, and removal of microbes from surfaces, synthesis of functionalized nanoparticles, antiscaling and surfactant mediated corrosion inhibitors, photocatalytic degradation of hazardous microbes, and nanotoxicity. He has published more than 400 technical papers and has been awarded over 25 patents. He is a member of the U.S National Academy of Engineering.